

The Performance of Time Reversal in an Elastic Cavity as a Function of Volume

Paige Elizabeth Simpson

A thesis submitted to the faculty of

Brigham Young University

In partial fulfillment of the requirements for the degree of

Bachelor of Science

Brian E. Anderson, Advisor

Department of Physics and Astronomy

Brigham Young University

June 2020

Copyright © 2020 Paige Simpson

All Rights Reserved

ABSTRACT

The Performance of Time Reversal in an Elastic Cavity as a Function of Volume

Paige Elizabeth Simpson

Department of Physics and Astronomy

Bachelor of Science

Time reversal may be used as an energy-focusing technique. It is applied in many different ways including, for example, nondestructive evaluation (NDE) of cracks in structures, reconstructing a source event, and providing an optimal carrier signal for communication. In NDE applications, it is often of interest to study small samples or samples that do not lend themselves to the bonding of transducers to their surfaces. A reverberant cavity, called a chaotic cavity, attached to the sample of interest provides space for the attachment of transducers as well as a more reverberant environment, which is critical to the quality of time reversal focusing. Transducers are attached to the chaotic cavity which is attached to the sample under test. The goal of this research is to explore the dependence of the quality of the time reversal focusing on the size of the chaotic cavity used. An optimal chaotic cavity will produce the largest focusing amplitude, best spatial resolution, and most linear focusing of the time reversed signal. This thesis shows experimentally that as the size of an aluminum rectangular chaotic cavity increases, the peak amplitude of the time-reversed focus tends to increase as well.

Keywords: Time reversal, chaotic cavity, elastic cavity, nondestructive evaluation

Acknowledgments

First and foremost, I would like to thank the College of Physical and Mathematical Sciences for funding this research and making it possible for me to work as research assistant for my time here at college.

Second, I would like to thank Dr. Brian Anderson for accepting me into his research group and tirelessly teaching me about time reversal and how to be a researcher.

Next, I would like to thank Sarah Young for her mentorship, friendship, and instruction manuals she left behind for me and all else who come afterward.

I would also like to thank those students who came before me researching time reversal; the bibliographies of your papers and theses made literature reviews and citations so much easier than they otherwise would have been.

Finally, I would like to thank my parents, siblings, fiancé, other family, and friends for their endless support of my endeavors; I would not have made it through college without you.

Table of Contents

Table of Contents	vi
List of Figures.....	viii
Chapter 1 Introduction	1
1.1 Time Reversal	1
1.2 Chaotic Cavities	2
1.3 Previous Work	4
1.4 Overview.....	5
Chapter 2 Methods.....	7
2.1 Experimental Setup	7
2.2 Time Reversal Methods.....	9
2.3 Sample Experiment and Result.....	10
2.4 Analysis Quantification Metrics.....	13
Chapter 3 Results.....	16
3.1 Results and Analysis.....	16
3.2 Comparison with Time Reversal in Rooms	19
Chapter 4 Conclusions	21
4.1 Conclusions.....	21
4.2 Directions for Further Work	21
Index.....	23

Bibliography.....24

List of Figures

Figure 2.1 Photograph of the rectangular chaotic cavity positioned under the laser vibrometer (not pictured). On the top surface of the cavity is a layer of reflective tape. Piezoelectric transducers are epoxied to the sides of the cavity.....	8
Figure 2.2 The red dot of laser light on the block is the focal position of these time reversal experiments. This position was chosen in order to avoid symmetries—it is not directly in line with any of the transducers and avoids the geometric center of the surface of the block.	11
Figure 2.3 Amplitude vs. time at the focal location for the four different types of time reversal.	13
Figure 3.1 Volume of the rectangular prism vs. peak amplitude using traditional time reversal. The peak amplitude of the time-reversed focus mostly increases as the volume of the chaotic cavity increases. There is a strong positive correlation between volume and peak amplitude of 0.79.....	17
Figure 3.2 A_p vs. volume for all four TR methods with amplitude linearly scaled to 100 mV for each metric.....	18

Chapter 1 Introduction

1.1 Time Reversal

Time reversal (TR) is a signal processing method^{1,2} that has three main uses: reconstructing a source event^{3,4,5,6}, providing an optimal carrier signal for communication^{7,8,9}, and intentionally focusing high energy waves to a point in space^{10,11,12}. TR can be performed in a bounded elastic medium, e.g. a block, using a source and a sensor¹³. By placing the sensor on one part of the block and the source on another, an impulse can be sent through the source and the response recorded at the sensor. The signal collected over time at the sensor is called the impulse response (IR). The IR first consists of an arrival corresponding to the impulse traveling directly from the source to the sensor (direct sound), followed by many arrivals of the impulse that reflected off of the boundaries and then reached the sensor (early and late reflections). If the recorded IR is flipped in time and broadcast in reverse, the late reflections are emitted first, then the early reflections, and finally the direct sound. Keeping the source and sensor in the same locations and sending this reversed impulse response (RIR) through the source will produce a TR focus approximating a reconstruction of the original impulse, but at the sensor instead of the source.

There are many different examples of TR being used in elastic media for nondestructive evaluation (NDE)^{14,15,16,17,18,19,20}. In NDE applications, sources are placed at fixed locations and a region of interest on the surface of the sample is selected. A laser may be used as the sensor, shined at several points within the region of interest. A full TR experiment is conducted at each sensor location and the nonlinear amplitude dependence of the TR focusing can be used to identify damage or delaminations. This type of experiment is called the time reversed elastic nonlinearity diagnostic (TREND). TR has been used in elastic media to locate earthquakes^{21,22} and for touchpad technology^{23,24}. It is also used in fluid media such as in room acoustics^{25,26,27,12,28}, biomedical applications^{29,30,31,32}, and underwater applications^{8,9,33}.

The purpose of this thesis is to explore the performance of TR used to focus elastic wave energy to a point in space as a function of volume. TR is performed in an aluminum rectangular block and the spatial dependence of the focusing is measured with a scanning laser Doppler vibrometer. This process is repeated for several different volumes as some of the block's volume is removed after each set of scans. This research will help to optimize the size of a chaotic cavity used in TR experiments for NDE applications.

1.2 Chaotic Cavities

In order to enhance the use of TR for NDE, a chaotic cavity may be used in the setup^{34,35,36,37}. Chaotic cavities are generally irregular shapes that are used in NDE applications of TR in order to increase peak amplitude (A_p) of TR focusing due to the addition of more reverberation in the IRs. A chaotic cavity is attached (i.e. glued/epoxied) to the sample under test. Also attached to the chaotic cavity is the source(s) that broadcasts ultrasound into the structure. Chaotic cavities are useful when the sample under test is too small to attach

transducers to, when it is undesirable to attach transducers to the sample under test, or when the sample under test has a relatively high amount of attenuation (e.g. wood, plastic) and thus not much internal reverberation.

Montaldo *et al.*³⁴ introduced the idea of using a chaotic cavity though they termed it a kaleidoscope. They asserted that chaotic cavities can be used to reduce side lobes. Their chaotic cavity was a cube with a partial sphere drilled out of one of the corners. One surface of their cavity was placed in contact with water so that energy focusing could be obtained within the water.

As previously mentioned, an aluminum rectangular block was used in this research and cut down to ten different volumes. The peak amplitude, temporal symmetry, temporal quality, spatial quality, spatial clarity, and the spatial full width at half maximum are quantified to explore the quality of the TR focusing as a function of volume. A rectangular prism was used instead of an irregular shape because it is a convenient shape to use in TR experiments. The rectangular cavity may not technically be considered a chaotic cavity, but it offers insight into the optimal cavity size used for the same purpose as a chaotic cavity is used for. Experiments conducted on a cylindrical volume have been completed but the data has not been processed yet and experiments to be conducted on a true chaotic, ergodic shaped cavity are currently in progress. Additionally, several TR processing techniques were explored, including traditional TR, deconvolution TR, clipping TR, and decay compensation TR. The cavities explored in this work were not used to couple reverberant energy into a second sample of interest. Rather it is assumed the higher quality time reversal, i.e. higher A_p and spatial confinement of the focusing, at a location on the cavity surface should translate to better coupling of energy into a sample of interest.

1.3 Previous Work

Willardson *et al.*¹² compared four different types of TR processing—traditional, decay compensation, deconvolution, and clipping for room acoustics application. Their experiments were done in a reverberation chamber with a loudspeaker and a microphone. Their goal was to figure out which type of TR gave the highest amplitude TR focus as well as the cleanest in terms of temporal quality. Willardson *et al.* found that clipping TR gave the highest A_p of the TR focus in a reverberation chamber though it did not provide the cleanest focus.

Young *et al.*¹⁹ used the same TR processing methods in solid media with the intent to detect cracks in structures. They used a fixed size chaotic cavity and compared five different types of TR in order to determine which method gave the highest amplitude of the focus with the least amount of negative side effects. Young *et al.* found that while the clipping method yielded the highest A_p , decay compensation TR was determined to be the best of the five methods for crack detection because it increased A_p over traditional TR and introduced the least amount of harmonics (a negative side effect of modifying the IR) compared to other TR methods. The clipping and one-bit TR methods introduce harmonic distortion simply due to the processing implemented.

Ribay *et al.*²⁵ studied TR in a room of fixed size and varied the absorption for different TR measurements. They found that A_p of the TR focus increased proportionally with reverberation time, τ , when the absorption was varied. Since τ is proportional to room volume it should follow that A_p will increase proportionally with increasing volume according to their results. They did not study how changing volumes of rooms changes the performance of TR.

Denison *et al.*²⁷ explored two types of changes to rectangular-shaped rooms and the resulting effects on TR performance. They studied the effect on A_p of the TR focus in rooms of different volumes but with the same absorption properties as well as identical-sized rooms with different amounts of absorption. Their work confirmed the findings of Ribay *et al.*²⁵ when the volume of the room was kept constant and the absorption was changed—as they decreased the absorption of the room to increase τ , the A_p increased proportionally. However, when Denison *et al.* changed the volume of the room while keeping the absorption the same, they discovered that A_p was proportional to $e^{-\tau}$ (meaning A_p decreases with increasing volume and with increasing τ) which is contrary to Ribay *et al.*'s assertion.

This research essentially combines what Young *et al.*¹⁹ and Denison *et al.*²⁷ have done. Four of the different types of TR that Young *et al.* explored in a single chaotic cavity shape were compared when conducted in a rectangular chaotic cavity. After each set of four TR methods was measured, the volume of the rectangular block was decreased, and the same measurements were repeated again. This was repeated until ten different volumes were measured. We studied the effect that volume of the chaotic cavity and type of TR method have on A_p and spatial extent at the TR focus.

1.4 Overview

In Chapter 2, the following are discussed: the experimental methods used including details of the experimental setup, the difference between the different TR methods, a sample experiment and result, and the metrics used to quantify and analyze this data. Chapter 3 includes results as a function of volume, the analysis thereof, as well as a discussion of the results in

comparison to TR in rooms as a function of volume. Chapter 4 offers conclusions and suggests further work to be done regarding chaotic cavities in TR studies.

Chapter 2 Methods

2.1 Experimental Setup

A Scanning Laser Doppler Vibrometer (SLDV), PSV-400, was used to measure the vibrations on the surface of the block. This was connected to a Polytec OFV-5000 Controller which has the velocity output connected to a 14-bit resolution, National Instruments PXI 5122 Digitizer card housed in a National Instruments PXI 1082 chassis. Also in the chassis, was a PXI 7852R Generator card with 4 channels connected to a 50-times gain, Tegam 9400 Power Amplifier. The outputs of the amplifier were connected to APC International piezoelectric transducers of type 851, diameter of 15.70 mm and thickness of 6.40 mm, that were polarized perpendicular to the electrodes. The transducers are epoxied to the chaotic cavity which can be seen in Fig. 2.1. The chaotic cavity is positioned under the SLDV with the cavity surface to be scanned located at a height of 26.5 ± 0.1 cm above the optical table, which is 93.5 ± 0.1 cm between the top of the chaotic cavity and the front edge of the SLDV head. The chaotic cavity has a layer of reflective tape on the scanning surface (see Fig. 2.1). This provides an optimal

reflecting surface for the laser light to be reflected back with enough strength into the SLDV to provide a low degree of background noise.

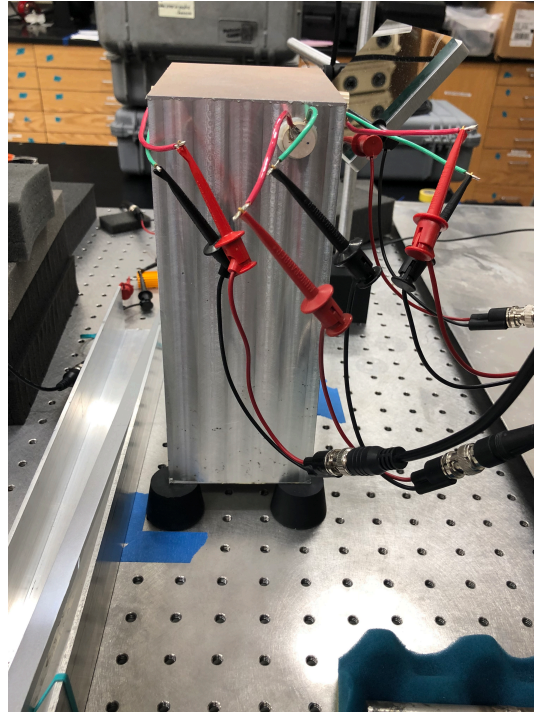


Figure 2.1 Photograph of the rectangular chaotic cavity positioned under the laser vibrometer (not pictured). On the top surface of the cavity is a layer of reflective tape. Piezoelectric transducers are epoxied to the sides of the cavity.

The initial dimensions of the rectangular chaotic cavity were 24.0 x 9.4 x 12.0 cm. After each set of experiments, the cavity was cut down to reduce the height (the dimension cut was that which initially measured 24.0 cm) by 2.1 cm with each cut. The smallest cavity measured 5.0 x 9.4 x 12.0 cm. The transducers remained fixed at the same locations each time the block was cut and the focal location was always at the same location (care was taken to ensure this). The density of the aluminum used was calculated to be 2824 kg/m³. The precise type(s) of waves used in these experiments was not determined but it is assumed that the spatial extent of the focusing is dominated by the Rayleigh wave speed and the depth of the focusing would be dominated by the shear wave speed, since the frequencies employed, cavity dimensions, and cavity material are very similar to those used by Remillieux *et al.*³⁸ The dominant Rayleigh wave

speed is approximately 2910 m/s and the central frequency wavelength is approximately 29.1 mm for 100 kHz.

2.2 Time Reversal Methods

Four different types of time reversal processing methods are explored here: traditional, deconvolution, clipping, and decay compensation. Traditional TR is just the IR flipped in time; there are no other modifications made to the signal response other than normalizing the RIR before amplifying it. The other three types of TR utilize modified versions of the IR.

Deconvolution TR, or inverse filtering TR, is a method which results in a temporally clean TR focus signal that has hardly any temporal side lobes^{39,40,41}. However, A_p is greatly reduced in amplitude to achieve that clean focal signal. The purpose of deconvolution TR is to minimize of the effects of system resonances in the “matched signal” TR process. One-bit TR⁴² (not explored in this paper) is a process in which the data samples in the RIR are set to be either 1 or -1. One-bit TR preserves the phase information in the RIR (the timing of the reflections) but provides a TR focusing signal with a high A_p and large side lobes. Clipping TR is a slight variant of one-bit TR, in which a threshold is defined such that all values below the chosen threshold maintain their original amplitudes and all values above the threshold are set equal to the threshold⁴³. Thus, the low-amplitude portion of the RIR, which has a lower signal-to-noise ratio, is not amplified by as much as the higher amplitude portion of the RIR that has a larger signal-to-noise ratio. Clipping TR produces a focal signal that is similar to one-bit TR but with a higher A_p . Clipping TR used here employed a threshold of 0.2 as suggested by Young *et al.*¹⁹ Decay compensation TR compensates for the exponential decay of the impulse response by using the envelope of the

RIR^{44,12,19}. In order to achieve this goal, the envelope is inverted, can be smoothed, and then multiplied by the RIR point by point. Thus, the modified RIR is amplified in a similar manner to one-bit or clipping but the tops of the signal have not been clipped as dramatically, hence why less harmonic distortion is introduced in decay compensation TR than with one-bit TR or clipping TR.

2.3 Sample Experiment and Result

Once the rectangular prism was set up beneath the SLDV, a spot was chosen on the block for the TR focus location. This spot, which can be seen in Fig. 2.2, was chosen in order to not be directly in line with any of the transducers and avoid the geometric center of the surface of the block to avoid any glaring symmetries in the TR focusing.

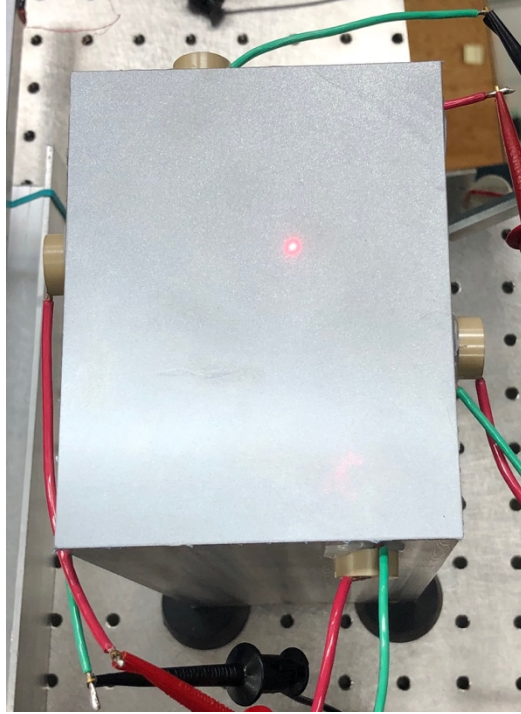


Figure 2.2 The red dot of laser light on the block is the focal position of these time reversal experiments. This position was chosen in order to avoid symmetries—it is not directly in line with any of the transducers and avoids the geometric center of the surface of the block.

A linear chirp signal spanning 75 kHz to 125 kHz is used in the forward step with an input voltage of 750 mV in order to extract the IR (through a cross correlation operation)^{28,45} between each transducer and the selected focus location. Those IR signals were reversed in time and sent through the respective transducers with an input voltage of 250 mV for traditional TR (100 mV for clipping TR and decay compensation TR, 1 V for deconvolution TR) to create the TR focus at the selected focus location (see Fig. 2.2). The TR focusing was assumed to be done at sufficiently low amplitudes that linear scaling would be expected. Thus, the differences in input voltages for the broadcast of the reversed IRs were accounted for (removed through linear scaling) when computing the TR focusing. These RIR signals were sent through the transducers multiple times, for averaging purposes (50 averages were used) and while the SLDV measured

the velocity response at various scan points on the block surface to measure the spatial dependence of a single TR focus. The scan grid included 65x52 points with a spacing of approximately 2 mm between each adjacent scan point. The spacing between scan points is approximately equal to $1/15^{\text{th}}$ of a wavelength.

After the data was collected from the scan, it was processed using MATLAB to calculate the TR quality quantification metrics described below. Results from a sample experiment can be seen in Fig. 2.3. The results shown in Fig. 2.3 are plots of the amplitude vs. time at the focal location for the four different types of TR. These results are from measurements taken on volume 8 of the rectangular block, which had dimensions of 9.2 x 9.4 x 12.0 cm. Deconvolution TR gives the cleanest signal but has the lowest amplitude. Clipping TR gives the highest A_p but has high amplitude side lobes.

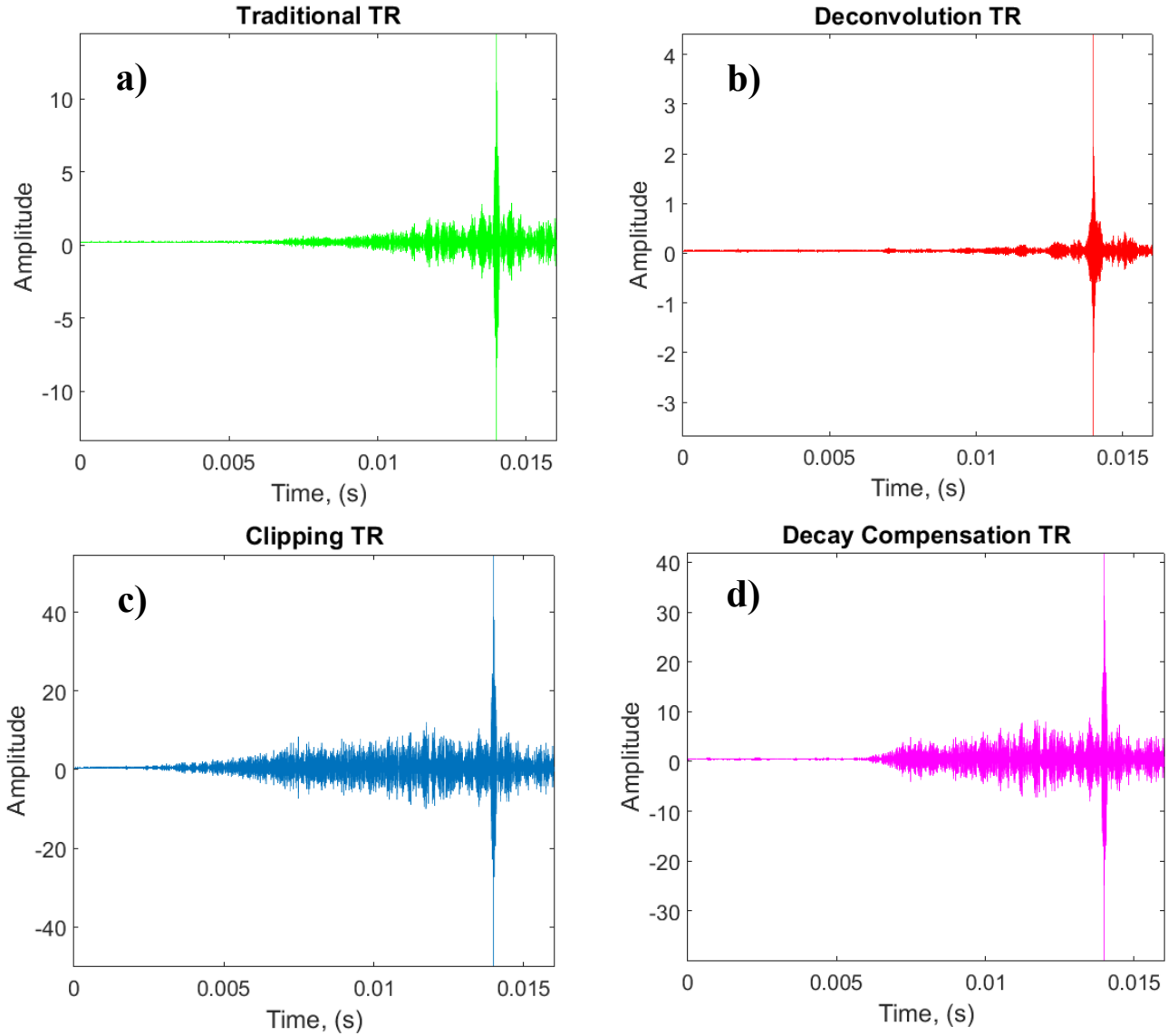


Figure 2.3 Amplitude vs. time at the focal location for the four different types of time reversal.

2.4 Analysis Quantification Metrics

The main metric of interest in the use of a chaotic cavity for NDE is the A_p of the TR focus. By changing the size of the rectangular block and repeating the experiments, the hope is to determine the relationship between A_p and cavity volume. Additional metrics such as temporal quality^{27,43}, spatial clarity²⁷, spatial quality⁴³, temporal symmetry⁴⁶, Heisenberg time^{27,47,48}, and spatial full width at half maximum (FWHM) all help to characterize the TR focal signal.

Temporal quality, ξ_T , is a metric that compares A_p^2 to the sum of the squared amplitudes in the rest of the samples in the focal signal (see Eq. (4) in reference 27). Here we remove the $1/M$ factor so that the ξ_T does not depend on the number of samples in the focal signal and is instead bound between values of 0 and 1. The perfect TR focal signal would be a delta function, which would have $\xi_T = 1$. The higher the ξ_T , the cleaner the temporal focal signal is because the side lobes are relatively small in amplitude compared to A_p .

Spatial clarity, Λ_S , compares the ξ_T at the focal location to the ξ_T of the rest of the scan points to show how significant the impulsive focusing is at the focus location. See Eq. (5) of reference 27. Again, we remove the $1/(N_x N_y)$ factor here so that Λ_S does not depend on the exact number of scan points used. Some of the scan points were off of the surface of the cavity. We zeroed out the amplitudes in these signals so that they would not impact the TR quality metric calculations. Removing this factor also ensures that Λ_S is bound between 0 and 1.

Spatial quality, ξ_S , compares A_p^2 to the sum of the squared amplitudes elsewhere in space at the time of the A_p . This metric is similar in purpose to the Λ_S metric except that the spatial evaluation is only considered at one point in time. See Eq. (7) in reference 43. Here again we remove the factor $1/(N_x N_y)$ such that ξ_S does not depend on the number of scan points used and is bound between 0 and 1.

Temporal symmetry, Σ_T , is a measure of the similarity of the portion of the focal signal before the time of A_p to the portion of the focal signal after the time of A_p . TR is known to be a temporally symmetric process, so the higher the degree of symmetry, the higher the quality of TR focusing. A perfectly symmetric signal would have a $\Sigma_T = 1$.

Heisenberg time is calculated for each volume of the chaotic cavity and is related to the modal density and the spacing between modal frequencies. A more detailed description is given in Chapter 3. Essentially the calculated Heisenberg time is longer than τ and the acquisition time for recording the IRs and the focal signals, meaning that the wave fields used in these experiments can be considered diffuse.

The spatial dependence of the focusing at the focal time of A_p was determined for a horizontal slice and a vertical slice through the map of the amplitude over all space at the focal time. The full width at half maximum (FWHM) of the squared amplitudes in each slice was then averaged. This metric gives insights into the spatial resolution of the focusing. In diffraction theory, the FWHM cannot be smaller than a half wavelength.

Chapter 3 Results

3.1 Results and Analysis

The A_p is extracted from the focal signal after applying a custom interpolation technique that employs zero padding to obtain a solid estimate of A_p by avoiding issues related to discrete quantization of samples. The A_p as a function of volume is plotted in Fig. 3.1 for traditional TR. There is a strong positive correlation coefficient of $r = 0.79$ for the traditional TR method between the volume of the chaotic cavity and A_p of the TR focus. This implies that as volume increases, A_p increases also. There are some fluctuations in the data of A_p as a function of volume. These fluctuations likely stem from the normalization procedure employed. The RIRs were normalized with respect to their peak amplitudes, and the peak amplitudes of these RIRs may not correspond to the direct sound, which should remain the same for each volume.

As far as the other metrics go for traditional TR, spatial clarity, spatial quality and temporal symmetry have moderate positive correlations with volume of the chaotic cavity; FWHM has a weak positive correlation with volume; and temporal quality has a very weak negative correlation with volume.

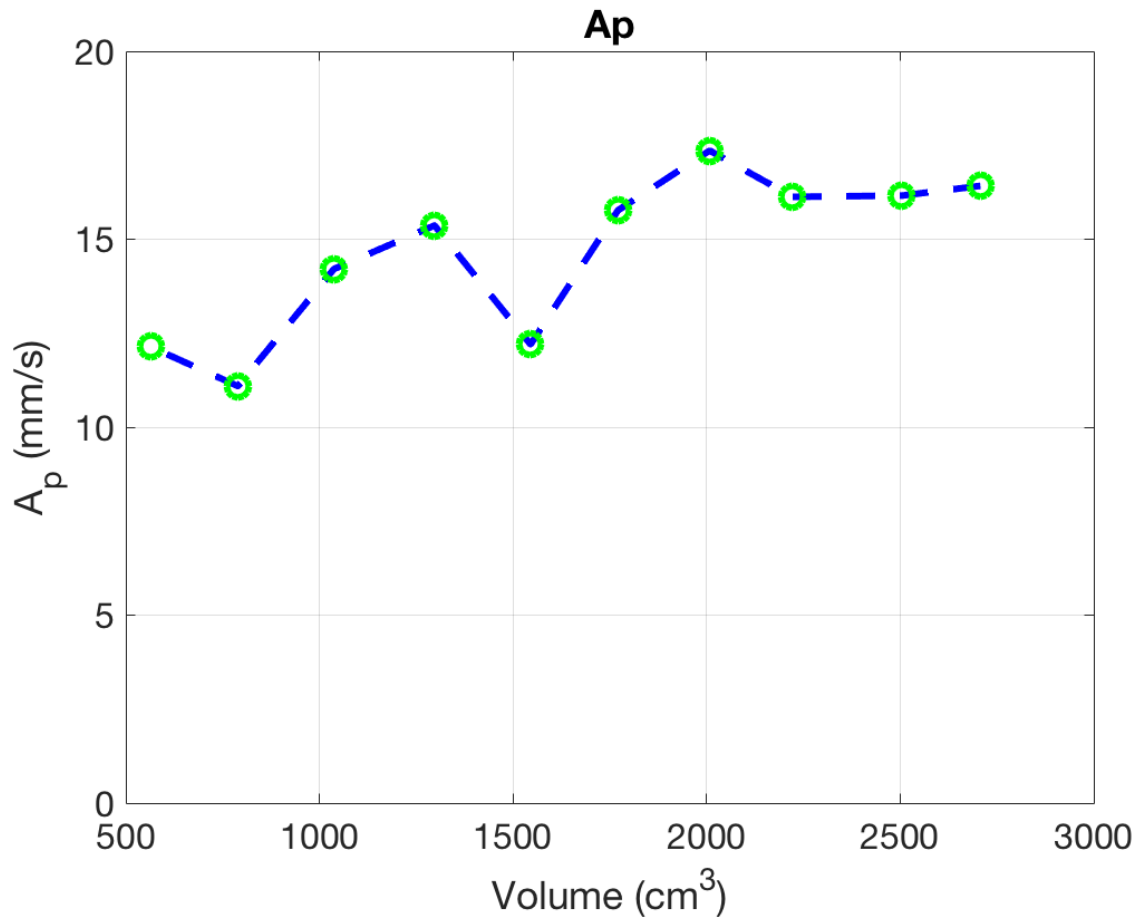


Figure 3.1 Volume of the rectangular prism vs. peak amplitude using traditional time reversal. The peak amplitude of the time-reversed focus mostly increases as the volume of the chaotic cavity increases. There is a strong positive correlation between volume and peak amplitude of 0.79.

Temporal symmetry has an average of .96 which is very close to 1. High symmetry speaks to a high-quality TR focus. While there is some correlation of these metrics with the volume of the sample, the spatial and temporal dependence of the focusing do not strongly depend on the cavity volume, at least for the range of cavity volumes explored here. If anything, the largest volume has the highest A_p and the highest quality spatial and temporal focusing.

For the rest of the TR methods, and including traditional TR, the metrics generally improve with larger volume. Fig. 3.2 shows the A_p vs. volume for all four TR methods with amplitude linearly scaled to 100 mV for each metric. This figure shows that, generally, A_p

increases with increased volume.

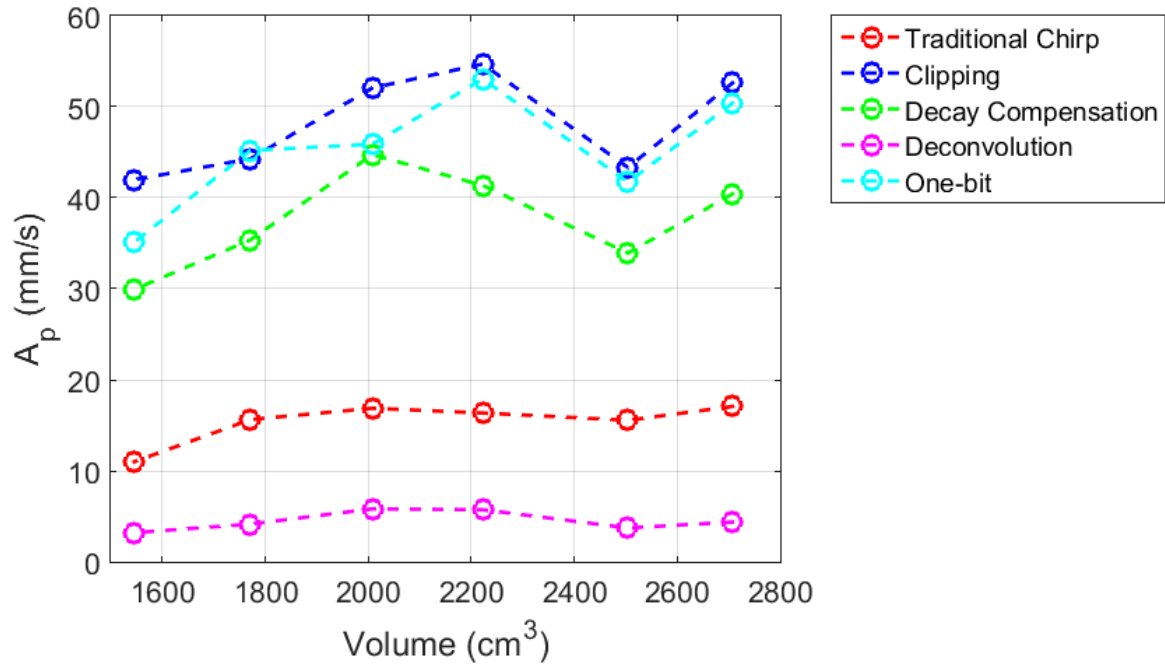


Figure 3.2 A_p vs. volume for all four TR methods with amplitude linearly scaled to 100 mV for each metric.

The Heisenberg time, t_H , is proportional to the modal density^{34,36,48}. Thus, the longer t_H is the more diffuse the wave field because the modal density is higher. Weaver indicates that if the duration of the experimental acquisition time is longer than t_H then it is as if the acoustic system has resolved each of the discrete modes⁴⁹. This means that waves have transited every portion of the sample and waves can only retrace paths they have already traveled. It is thus not useful to record an impulse response longer in duration than t_H . For an elastic medium, t_H varies with volume, surface area, and frequency. The shortest t_H we calculated, based on a derivative with respect to frequency of an equation for the number of modes in an elastic cavity given by Weaver⁵⁰, was 25.5 ms for 75 kHz and for the smallest volume tested. This time of 25.5 ms is

longer than the acquisition time and is longer than the reverberation time. For the largest volume, $t_H = 106$ ms, and again the acquisition time and reverberation times were smaller than this value. Thus, it is reasonable to assume that wave field in each of our rectangular cavity volumes is diffuse and the modes are not yet resolved.

3.2 Comparison with Time Reversal in Rooms

The finding of an increase in A_p with increasing volume in the TR experiments conducted on the different volumes of the rectangular aluminum block seems to agree with the assertion of Ribay *et al.*²⁵ and disagree with the findings of Denison *et al.*²⁷ Our data shows that increasing volume of the chaotic cavity increases the peak amplitude of the TR focus. Ribay *et al.*'s research showed that as absorption of one room was decreased (volume constant), A_p and τ increased but they made a general statement that A_p is proportional to τ and didn't explicitly show how A_p should change when room volume is changed. Denison *et al.* showed that as the volume of the room increased (absorption constant), A_p followed the relationship $e^{-\tau}$. Because τ is proportional to room volume for sound in air, the work of Denison *et al.* suggests that as volume is increased that the A_p should decrease. The research presented here observed the relationship between A_p vs. volume. However, Ribay *et al.* and Denison *et al.* observed the relationship of A_p vs. τ . Because τ is proportional to volume for sound in rooms, it is very likely that a similar relationship holds for bounded elastic media. It is possible that the discrepancy of our findings with that of Denison *et al.* is because the experiments here were conducted with elastic waves whereas the work of Ribay *et al.* and Denison *et al.* were done with sound in rooms. We expected the results of this experiment to be similar to Denison *et al.*'s findings

because the process was similar of just changing the volume and keeping everything else the same. However, loss of wave energy in rooms is mostly due to wall absorption and spherical spreading, but loss of wave energy in solids is due to propagation losses in addition to boundary reflection losses and spherical spreading. Further work may determine whether the differences in the results have to do with differences in losses for waves in solids and sound in air or whether the differences may be due to some other effect.

Chapter 4 Conclusions

4.1 Conclusions

There is a strong positive correlation between the volume and peak amplitude for the solid rectangular chaotic cavity. The findings here may not be very comparable to Denison *et al.*'s because volume may be coupled with absorption in solids thus making it impossible to change one without changing the other. This research suggests that the bigger the chaotic cavity used, the better the peak amplitude of the TR focus will be. If nothing else, a bigger chaotic cavity would allow more room to attach more sources, and more sources definitely means a higher A_p .

4.2 Directions for Further Work

This work only explored different volumes of one rectangular prism. To further explore chaotic cavities used in time reversal, one could consider studying several other shapes and varying the volume such as was done with the rectangular prism here. Another shape to consider would be a cylindrical prism because the waves bouncing around a cylindrical prism might be more random than that of a rectangular prism. Another more important shape to measure would

be an ergodic cavity. An ergodic shape is one that avoids symmetries and parallel walls⁴⁸. Many researchers claim that an ergodic cavity is necessary because the waves are the most randomized when it is used. Comparing an ergodic chaotic cavity against these other two would help shed light on the subject of whether or not going to the lengths to make an ergodic chaotic cavity is necessary for TR experiments.

Another idea to consider for further work would be to change the source location and scan area proportionally when changing the volume. This would keep the sources and receivers in the same place proportional to the size of the block. This could potentially introduce fewer variables when comparing between volumes since each volume would look exactly the same, just scaled.

Index

C

chaotic cavity · iii, 2, 5, 7, 16

cylindrical prism · 21

E

ergodic · 22

N

Nondestructive Evaluation · i, iii

R

rectangular prism · 3, 10, 13, 17

T

Time reversal · 1

Time Reversal · i, iii, 1, 9, 19

traditional chirp · 13, 17

Bibliography

-
- ¹ M. Fink, "Time reversed acoustics," *Phys. Today* **50**(3), 34-40 (1997).
- ² B. E. Anderson, M. Griffa, C. Larmat, T.J. Ulrich, and P.A. Johnson, "Time reversal," *Acoust. Today*, **4** (1), 5-16 (2008).
- ³ M. Scalerandi, A.S. Gliozzi, B.E. Anderson, M. Griffa, P.A. Johnson, and T.J. Ulrich, "Selective source reduction to identify masked sources using time reversal acoustics," *J. Phys. D Appl. Phys.* **41**, 155504 (2008).
- ⁴ B.E. Anderson, T.J. Ulrich, M. Griffa, P.-Y. Le Bas, M. Scalerandi, A.S. Gliozzi and P.A. Johnson, "Experimentally identifying masked sources applying time reversal with the selective source reduction method," *J. Appl. Phys.* **105**(8), 083506 (2009).
- ⁵ C.S. Larmat, R.A. Guyer, and P.A. Johnson, "Time-reversal methods in geophysics," *Physics Today* **63**(8), 31-35 (2010).
- ⁶ B.E. Anderson, M. Griffa, T.J. Ulrich, and P.A. Johnson, "Time reversal reconstruction of finite sized sources in elastic media," *J. Acoust. Soc. Am.* **130**(4), EL219-EL225 (2011).
- ⁷ B. E. Anderson, T. J. Ulrich, P.-Y. Le Bas, and J. A. Ten Cate, "Three dimensional time reversal communications in elastic media," *J. Acoust. Soc. Am.* **139**(2), EL25-EL30 (2016).
- ⁸ H. C. Song, "An Overview of Underwater Time-Reversal Communication," *IEEE Journal of Oceanic Engineering*, **41**(3), 644-655 (2016).
- ⁹ L. P. Maia, A. Silva and S. M. Jesus, "Environmental Model-Based Time-Reversal Underwater Communications," in *IEEE Access*, **6**, 10041-100051 (2018).
- ¹⁰ P.-Y. Le Bas, T.J. Ulrich, B.E. Anderson, and J.J. Esplin, "A high amplitude, time reversal acoustic non-contact excitation (TRANCE)," *J. Acoust. Soc. Am.* **134**(1), EL52-EL56 (2013).
- ¹¹ B.E. Anderson, M.C. Remillieux, P.-Y. Le Bas., T.J. Ulrich (2019) Time Reversal Techniques. In: Kundu T. (eds) Nonlinear Ultrasonic and Vibro-Acoustical Techniques for Nondestructive Evaluation. Springer, Cham.
- ¹² M. L. Willardson, B. E. Anderson, S. M. Young, M. H. Denison, and B. D. Patchett, "Time reversal focusing of high amplitude sound in a reverberation chamber," *J. Acoust. Soc. Am.* **143**(2), 696-705 (2018).
- ¹³ A.M. Sutin, J.A. TenCate, and P.A. Johnson, "Single-channel time reversal in elastic solids," *J. Acoust. Soc. Am.* **116**(5), 2779-2784 (2004).
- ¹⁴ T.J. Ulrich, P.A. Johnson, and A. Sutin, "Imaging nonlinear scatterers applying the time reversal mirror," *J. Acoust. Soc. Am.* **119**, 1514-1518 (2006).
- ¹⁵ T.J. Ulrich, P.A. Johnson, and R.A. Guyer, "Interaction dynamics of elastic waves with a complex nonlinear scatterer through the use of a time reversal mirror," *Phys. Rev. Lett.* **98**, 104301 (2007).
- ¹⁶ T.J. Ulrich, A.M. Sutin, T. Claytor, P. Papin, P.-Y. Le Bas, and J.A. TenCate, "The time reversed elastic nonlinearity diagnostic applied to evaluation of diffusion bonds," *Appl. Phys. Lett.* **93**, 151914 (2008).

-
- ¹⁷ B.E. Anderson, M. Griffa, T.J. Ulrich, P.-Y. Le Bas, R.A. Guyer, and P.A. Johnson, "Crack localization and characterization in solid media using time reversal techniques," *Am. Rock Mech. Assoc.*, #10-154 (2010).
- ¹⁸ B.E. Anderson, M. Griffa, P.-Y. Le Bas, T.J. Ulrich, and P.A. Johnson, "Experimental implementation of reverse time migration for nondestructive evaluation applications," *J. Acoust. Soc. Am.* **129**(1), EL8-EL14 (2011).
- ¹⁹ S. M. Young, B. E. Anderson, M. L. Willardson, P. E. Simpson, and P.-Y. Le Bas, "A comparison of impulse response modification techniques for time reversal with application to crack detection," *J. Acoust. Soc. Am.* **145**(5), 3195-3207 (2019).
- ²⁰ S. M. Young, B. E. Anderson, S. M. Hogg, P.-Y. Le Bas, and M. C. Remillieux, "Nonlinearity from stress corrosion cracking as a function of chloride exposure time using the time reversed elastic nonlinearity diagnostic," *J. Acoust. Soc. Am.* **145**(1), 382-391 (2019).
- ²¹ C. Larmat, J.-P. Montagner, M. Fink, Y. Capdeville, A. Tourin, E. Clevede, "Time-reversal imaging of seismic sources and applications to the great Sumatra earthquake," *Geophys. Res. Lett.* **33**, L19312 (2006).
- ²² C. Larmat, J. Tromp, Q. Liu, J.-P. Montagner, "Time-Reversal location of glacial earthquakes," *J. Geophys. Res.*, **113**(B9), B09314. (2008).
- ²³ R. K. Ing, N. Quieffin, "In solid localization of finger impacts using acoustic time-reversal process," *Appl. Phys. Lett.* **87**(20), 204104 (2005).
- ²⁴ D. Vigoureux, J.-L. Guyader, "A simplified Time Reversal method used to localize vibrations sources in a complex structure," *Appl. Acoust.* **73**(5), 491-496 (2012).
- ²⁵ G. Ribay, J. de Rosny, and M. Fink, "Time reversal of noise sources in a reverberation room," *J. Acoust. Soc. Am.*, **117**(5), 2866-28720 (2005).
- ²⁶ M. H. Denison and B. E. Anderson, "The effects of source placement on time reversal focusing in rooms," *Appl. Acoust.* **156**, 279-288 (2019).
- ²⁷ M. H. Denison and B. E. Anderson, "Time reversal acoustics applied to rooms of various reverberation times," *J. Acoust. Soc. Am.* **144**(6), 3055-3066 (2018).
- ²⁸ B. E. Anderson, M. Clemens, and M. L. Willardson, "The effect of transducer directionality on time reversal focusing," *J. Acoust. Soc. Am.* **142**(1), EL95-EL101 (2017).
- ²⁹ J.-L. Thomas, F. Wu, M. Fink, "Time reversal mirror applied to litotripsy," *Ultrason. Imag* **18**, 106-121 (1996).
- ³⁰ J.-L. Thomas, M. Fink, "Ultrasonic beam focusing through tissue inhomogeneities with a time reversal mirror: application to transskull therapy," *IEEE Trans. Ultrason. Ferroelect. Freq. Contr.* **43**(6), 1122-1129 (1996).
- ³¹ M. Tanter, J.-L. Thomas, M. Fink, "Focusing and steering through absorbing and aberating layers: application to ultrasonic propagation through the skull," *J. Acoust. Soc. Am.* **103**(5), 2403-2410 (1998).
- ³² S. Dos Santos, Z. Prevorovsky, "Imaging of human tooth using ultrasound based chirp-coded nonlinear time reversal acoustics," *Ultrasonics* **51**(6), 667-674 (2011).
- ³³ T. Shimura, Y. Watanabe, H. Ochi, and H. C. Song, "Long-range time reversal communication in deep water: Experimental results," *J. Acoust. Soc. Am.* **132**(1), EL49-EL53 (2012).
- ³⁴ G. Montaldo, D. Palacio, M. Tanter, and M. Fink, "Time reversal kaleidoscope: A smart transducer for three-dimensional ultrasonic imaging," *Appl. Phys. Lett.* **84**(19), 3879-3881 (2004).

-
- ³⁵ O. Bou Matar, S. Delrue, K. Van den Abeele. "Optimization of chaotic cavity transducers to nonlinear elastic imaging." Société Française d'Acoustique - SFA. 10ème Congrès Français d'Acoustique, Apr 2010, Lyon, France. 2010. <hal-00551140>
- ³⁶ N. Quieffin, S. Catheline, R. K. Ing and M. Fink, "2D pseudo-array using an ultrasonic one channel time-reversal mirror," IEEE Ultrasonics Symposium, 2004, Montreal, Quebec, Canada, 2004, pp. 801-804 Vol.1.
- ³⁷ C. Draeger, J-C. Aime, and M. Fink, "One-channel time reversal in chaotic cavities: Experimental results," *J. Acoust. Soc. Am.* **105**(2), 618-625 (1999).
- ³⁸ M. C. Remillieux, B. E. Anderson, T. J. Ulrich, P.-Y. Le Bas, and C. Payan, "Depth profile of a time-reversal focus in an elastic solid," *Ultrasonics* **58**, 60-66 (2015).
- ³⁹ M. Tanter, J.-L. Thomas, M. Fink, Time reversal and the inverse filter, *J. Acoust. Soc. Am.* **108** (2000) 223–234.
- ⁴⁰ T. Gallot, S. Catheline, P. Roux, M. Campillo, "A passive inverse filter for Green's function retrieval", *J. Acoust. Soc. Am.* **131** (2011) EL21–EL27.
- ⁴¹ B. E. Anderson, J. Douma, T. J. Ulrich, and R. Snieder, "Improving spatio-temporal focusing and source reconstruction through deconvolution," *Wave Motion* **52**, 151-159 (2015).
- ⁴² G. Montaldo, P. Roux, A. Derode, C. Negreira, M. Fink, "Ultrasound shock wave generator with one-bit time reversal in a dispersive medium, application to lithotripsy." *Appl. Phys. Lett.* **80**(5), 87–89 (2002).
- ⁴³ C. Heaton, B. E. Anderson, and S. M. Young, "Time reversal focusing of elastic waves in plates for educational demonstration purposes," *J. Acoust. Soc. Am.* **141**(2), 1084-1092 (2017).
- ⁴⁴ A. S. Gliozzi, M. Scalerandi, and P. Antonaci, "One-channel time-reversal acoustics in highly attenuating media," *J. Phys. D: Appl. Phys.* **46**, 135502 (2013).
- ⁴⁵ B. Van Damme, K. Van Den Abeele, Y. Li, and O. Bou Matar, "Time reversed acoustics techniques for elastic imaging in reverberant and nonreverberant media: An experimental study of the chaotic cavity transducer concept," *J. Appl. Phys.* **109**, 104910 (2011).
- ⁴⁶ T. J. Ulrich, M. Griffa, and B. E. Anderson, "Symmetry-based imaging condition in time reversed acoustics," *J. Appl. Phys.* **104**(6), 064912 (2008).
- ⁴⁷ N. Quieffin, "Etude du rayonnement acoustique de structures solides: Vers un système d'imagerie haute résolution" ("Study of the acoustic radiation of solid structures: towards a high resolution imaging system"), Ph.D. thesis, Université Pierre et Marie Curie, Paris, France (2004).
- ⁴⁸ R. Weaver, "The unreasonable effectiveness of random matrix theory for the vibrations and acoustics of complex structures," in *New Directions in Linear Acoustics and Vibration*, edited by M. Wright, and R. Weaver (Cambridge University Press, Cambridge, UK, 2010), Chap. 3, pp. 42–58 and 74-75.
- ⁴⁹ P. Sebbah, ed. *Waves and imaging through complex media*. Springer Science & Business Media, 2001.
- ⁵⁰ R. Weaver. "Spectral statistics in elastodynamics." *J. Acoust. Soc. Am.* **85**(3), pp. 1005-1013 (1989).